A NUMERICAL ALGORITHM FOR KINEMATIC ANALYSIS OF THE MACPHERSON STRUT SUSPENSION SYSTEM USING POINT COORDINATES

HAZEM ALI ATTIA

ABSTRACT. In the present paper, a numerical algorithm for the kinematic analysis of a MacPherson strut motor-vehicle suspension system is developed. The kinematic analysis is carried out in terms of the rectangular Cartesian coordinates of some defined points in the links and at the joints. The presented formulation in terms of this system of coordinates is simple and involves only elementary mathematics. The resulting constraint equations are mostly either linear or quadratic in the rectangular Cartesian coordinates. The proposed formulation eliminates the need to write redundant constraints and allows to solve a reduced system of equations which leads to better accuracy and a reduction in computing time. The algorithm is applied to solve the initial positions as well as the finite displacement, velocity and acceleration problems for the MacPherson strut motor-vehicle suspension system.

1. INTRODUCTION

In recent years various methods for the analytical and computational kinematic analysis of spatial mechanisms were developed. Such methods can be classified according to the type of coordinates chosen to determine their configuration and specify their constraints. Some formulations use a large set of absolute coordinates [1,2]. The position and orientation of any rigid link in the mechanism are described with respect to the global reference coordinate system. The algebraic equations of constraints are introduced to represent the kinematic joints that connect the rigid bodies. Although in this type of formulation the constraint equations are easy to construct, it has the disadvantage of the large number of defined coordinates. Other formulations use relative coordinates where the position of each link is defined with respect to the previous link

by means of relative joint coordinates that depend on the type of the joint used [3-5]. This type of formulation yields the constraints as a minimal set of algebraic equations. However, the constraint equations are derived based on loop closure equations, and the resulting constraint equations are highly nonlinear and contain complex circular functions. Another formulation which is based on point coordinates is discussed in [6-13]. The configuration of the system is described in terms of the rectangular Cartesian coordinates of some defined points in the links and at the joints. The system constraint equations are then written to fix the relative positions of the points in each rigid link and also the relative positions between the different links determined by the type of joints connecting them. In this paper the kinematic analysis of a MacPherson strut motor-vehicle suspension system is carried out in terms of point coordinates. The position, velocity, and acceleration analyses are carried out to determine the positions, velocities, and accelerations for the unknown points and links in the mechanism. The velocities and accelerations of other points of interest can also be calculated. The angular velocity and acceleration of any link in the mechanism are evaluated in terms of the Cartesian coordinates, velocities, and accelerations of the assigned points.

2. MODELLING OF THE MACPHERSON STRUT SUSPENSION

In the past ten years much attension has been focused on improving the ride/handling compromise of the car by using a multi-loop suspension and steering mechanism. The multi-loop structure usually gives the possibility to separate the wheel bouncing parameters determining ride comfort from steering. The MacPherson strut is being used for front wheel axles of current small cars, and can also be used for rear axles. The light weight and compact size of the mechanism are its main advantages. Furthermore, the system design allows longer axle springs, and thus a soft and long-strike suspension. Figure 1 illustrates the multi-loop MacPherson Strut suspension system mounted on the left side of the vehicle [5]. According to its performance, the mechanism can be separated into two independent parts; bouncing mechanism and steering mechanism (see Fig. 2 [5]). The bouncing mechanism consists of the four-bar linkage OAED with links 1, 2, 3, and 4. The bouncing action caused by the rotation of the lower arm (link 2) about the axis O_1, O_2 and the accompanying relative sliding motion of the portions of the strut (link 3 and 4). The lower portion of the strut is the wheel knuckle. The

steering mechanism consists of the four-bar linkage FCBD. The steering action caused by the sliding motion of the steering rack (link 6), and accompanying motion of the tie rod (link 5) causing the rotation of the strut about the steering axis AD. The joints at A, B, C and D are spherical joints, while the coaxial joints at O_1 and O_2 are revolute joints forming a compound revolute joint. The strut joint at E is a sliding joint with compliance. Thus, the MacPherson strut suspension mechanism consists of six links, four spherical joints and one compound revolute joint and two sliding joints. The system has three degrees-of-freedom (DOF): one DOF corresponding to the vertical motion of the chassis and two DOF associated with the four-bar linkages constituting the bouncing and steering mechanisms, one corresponds to the A-arm rotation and the later corresponds to the steering input.

2.1. Displacement Analysis. The configuration of the mechanism can be specified by defining the Cartesian coordinates of a set of points on the links and joints relative to a reference frame. Figure 3 illustrates the mechanism with the assigned points and the reference frame fixed to the chassis. The positive x-direction is taken to the rear of the vehicle; the positive y-direction is taken to the right of the vehicle parallel to the sliding axis of the steering rack at F; and the positive z-direction is thus taken in the vertical upwards. Each binary link is replaced by two points located at both ends, while the adjacent links are sharing common points. The strut sliding joint is represented by two pairs of points: (5, 7) and (4, 8) each is located at one of the sliding bodies to define the direction of the axis of the joint at any instant. The sliding joint F is represented by two points 3 and 9. Each of the four spherical joints is represented by one point located at its centre, i.e., points 4, 5, 6, and 9, while the compound revolute joint is represented by two points 1 and 2 located on its axis. The whole mechanism is then replaced by 9 points. These points are classified as known or unknown points. The known points are points 1, 2, 3 and 4 that are fixed on the chassis. The Cartesian coordinates of the five unknown points 5, 6, 7, 8 and 9 located on the moving links define the motion variables. Therefore, 15 constraint equations are needed to solve for the 15 unknown Cartesian coordinates. The constraints are either geometric or kinematic constraints. Geometric constraints are the distance constraints that fix the relative positions of the points located on the same rigid link of the mechanism. The geometric constraint equations are expressed in the Cartesian coordinates of the points

as follows,

$$(x_5 - x_1)^2 + (y_5 - y_1)^2 + (z_5 - z_1)^2 - d_{5,1}^2 = 0 \tag{1}$$

$$(x_5 - x_2)^2 + (y_5 - y_2)^2 + (z_5 - z_2)^2 - d_{5,2}^2 = 0 \tag{2}$$

$$(x_6 - x_5)^2 + (y_6 - y_5)^2 + (z_6 - z_5)^2 - d_{6,5}^2 = 0 \tag{3}$$

$$(x_7 - x_5)^2 + (y_7 - y_5)^2 + (z_7 - z_5)^2 - d_{7,5}^2 = 0 \tag{4}$$

$$(x_7 - x_6)^2 + (y_7 - y_6)^2 + (z_7 - z_6)^2 - d_{7,6}^2 = 0 \tag{5}$$

$$(x_8 - x_4)^2 + (y_8 - y_4)^2 + (z_8 - z_4)^2 - d_{8,4}^2 = 0 \tag{6}$$

$$(x_9 - x_6)^2 + (y_9 - y_6)^2 + (z_9 - z_6)^2 - d_{9,6}^2 = 0 \tag{7}$$

where $d_{i,j}$ is the distance between points i and j belonging to the same rigid link, and x_i, y_i, and z_i are the Cartesian coordinates of point i. Kinematic constraints result from the conditions imposed by the kinematic joints on the relative motion between the bodies they comprise. Points located at the centre of a spherical joint or at the axis of a revolute joint automatically eliminate all the kinematic constraints due to these joints. However, because of the presence of the strut sliding joint in the mechanism, kinematic constraints are added in terms of the coordinates of the points located along the axis of the strut sliding joint. Such kinematic constraints are expressed as,

$$(y_7 - y_5)(z_8 - z_4) - (z_7 - z_5)(y_8 - y_4) = 0 \tag{8}$$

$$(x_7 - x_5)(z_8 - z_4) - (z_7 - z_5)(x_8 - x_4) = 0 \tag{9}$$

$$(y_7 - y_4)(z_8 - z_4) - (z_7 - z_4)(y_8 - y_4) = 0 \tag{10}$$

$$(x_7 - x_4)(z_8 - z_4) - (z_7 - z_4)(x_8 - x_4) = 0 \tag{11}$$

Moreover, driving constrains are added to the above constraints as functions of the two driving variables, namely, the angle θ of the lower arm and the sliding variable S of the steering rack (see Fig. 3) in the form,

$$(z_5 - z_1) - d_{5,1}\cos(\theta) = 0 \tag{12}$$

$$x_9 - x_3 = 0 \tag{13}$$

$$y_9 - y_3 + S = 0 \tag{14}$$

$$z_9 - z_3 = 0 \tag{15}$$

Equation (1) expresses the required 15 independent constraint equations in terms of the Cartesian coordinates of the assigned points. Given the set of the known coordinates and the driving variables at each instant, the nonlinear constraint Eq. (1) can be solved by any iterative numerical method [14] to determine the 15 unknown Cartesian coordinates. The main kinematical properties of the suspension are described by the coordinates of the wheel centre point, the kingpin angle α and the camber angle β [15]. The wheel centre point (point 10, see Fig. 2) is defined as the point at which the wheel spin axis intersects the wheel plane. Points 7 and 10 define the wheel spin axis. The coordinates of the wheel centre point can easily be determined by specifying its position relative to three other points 5, 6, and 7 on the knuckle. The Kingpin angle determines the steering aligning torque in conjunction with steering offset and wheel caster. The kingpin angle α is defined as the inclination angle of the steering axis AD relative to the vertical longitudinal plane, measured in the transverse plane of the vehicle [14] and therefore from Fig. 4;

$$\alpha = \tan^{-1} \frac{(y_7 - y_5)}{(z_7 - z_5)} \tag{16}$$

A positive angle α signifies a displacement of point 5 in the negative y direction. The camber angle β is the inclination of the wheel plane relative to the longitudinal vehicle plane, measured in the transverse plane of the vehicle and therefore;

$$\beta = \tan^{-1} \frac{(z_7 - z_{10})}{y_7 - y_{10})} \tag{17}$$

Positive camber means that the wheels are tilted out at the top than at the bottom.

2.2. Velocity and Acceleration Analyses.

The velocity equations are derived by differentiating Eq. (1) with respect to time. Since the velocity equations are linear, the vector of velocities; $\dot{\mathbf{q}} = [\dot{q}_1, \dot{q}_2, \cdots q_{27}, \dot{S}, \dot{\theta}]^T$ can be partitioned; $\dot{\mathbf{q}} = [[u]^T, \dot{w}^T]^T$, and the velocity equation is written in the partitioned matrix form,

$$[C_q]\dot{\mathbf{q}} = 0 \tag{18}$$

$$[C_u]\dot{\mathbf{u}} = [C_w]\dot{\mathbf{w}} \tag{19}$$

where $\dot{\mathbf{u}} = [\dot{x}_5, \dot{y}_5, \dot{z}_5, \cdots, \dot{z}_9]^T$ and $\dot{\mathbf{w}} = [\dot{x}_1, \dot{y}_1, \dot{z}_1, \cdots, \dot{S}, \dot{\theta}]^T$ are the unknown and known vectors of velocities, respectively. Let $x_{i,j} = x_i - x_j$, then the two sub-matrices

$[C_u]$ and $[C_w]$ of the constraint Jacobian matrix $[C_q]$ which contains the partial derivatives of the constraint equations with respect to the points coordinates are;

$$[C_u] = \begin{bmatrix}
2x_{5,1} & 2y_{5,1} & 2z_{5,1} & 0 & 0 & 0 & 0 & 0 & 0 & 0 & 0 & 0 & 0 & 0 & 0 \\
2x_{5,2} & 2y_{5,2} & 2z_{5,2} & 0 & 0 & 0 & 0 & 0 & 0 & 0 & 0 & 0 & 0 & 0 & 0 \\
2x_{5,6} & 2y_{5,6} & 2z_{5,6} & 2x_{6,5} & 2y_{6,5} & 2z_{6,5} & 0 & 0 & 0 & 0 & 0 & 0 & 0 & 0 & 0 \\
2x_{5,7} & 2y_{5,7} & 2z_{5,7} & 0 & 0 & 0 & 2x_{7,5} & 2y_{7,5} & 2z_{7,5} & 0 & 0 & 0 & 0 & 0 & 0 \\
0 & 0 & 0 & 2x_{6,7} & 2y_{6,7} & 2z_{6,7} & 2x_{7,6} & 2y_{7,6} & 2z_{7,6} & 0 & 0 & 0 & 0 & 0 & 0 \\
0 & 0 & 0 & 0 & 0 & 0 & 0 & 0 & 0 & 2x_{8,4} & 2y_{8,4} & 2z_{8,4} & 0 & 0 & 0 \\
0 & 0 & 0 & 2x_{6,9} & 2y_{6,9} & 2z_{6,9} & 0 & 0 & 0 & 0 & 0 & 0 & 2x_{9,6} & 2y_{9,6} & 2z_{9,6} \\
0 & z_{4,8} & y_{8,4} & 0 & 0 & 0 & 0 & z_{8,4} & y_{4,8} & 0 & z_{5,7} & y_{7,5} & 0 & 0 & 0 \\
z_{4,8} & 0 & x_{8,4} & 0 & 0 & 0 & z_{8,4} & 0 & x_{4,8} & z_{5,7} & 0 & x_{7,5} & 0 & 0 & 0 \\
0 & 0 & 0 & 0 & 0 & 0 & 0 & z_{8,4} & y_{4,8} & 0 & z_{4,7} & y_{7,4} & 0 & 0 & 0 \\
0 & 0 & 0 & 0 & 0 & 0 & z_{8,4} & 0 & x_{4,8} & z_{4,7} & 0 & x_{7,4} & 0 & 0 & 0 \\
0 & 0 & 1 & 0 & 0 & 0 & 0 & 0 & 0 & 0 & 0 & 0 & 0 & 0 & 0 \\
0 & 0 & 0 & 0 & 0 & 0 & 0 & 0 & 0 & 0 & 0 & 0 & 1 & 0 & 0 \\
0 & 0 & 0 & 0 & 0 & 0 & 0 & 0 & 0 & 0 & 0 & 0 & 0 & 1 & 0 \\
0 & 0 & 0 & 0 & 0 & 0 & 0 & 0 & 0 & 0 & 0 & 0 & 0 & 0 & 1
\end{bmatrix} \tag{20}$$

and

$$[C_w] = \begin{bmatrix}
2x_{5,1} & 2y_{5,1} & 2z_{5,1} & 0 & 0 & 0 & 0 & 0 & 0 & 0 & 0 & 0 & 0 & 0 \\
0 & 0 & 0 & 2x_{5,2} & 2y_{5,2} & 2z_{5,2} & 0 & 0 & 0 & 0 & 0 & 0 & 0 & 0 \\
0 & 0 & 0 & 0 & 0 & 0 & 0 & 0 & 0 & 0 & 0 & 0 & 0 & 0 \\
0 & 0 & 0 & 0 & 0 & 0 & 0 & 0 & 0 & 0 & 0 & 0 & 0 & 0 \\
0 & 0 & 0 & 0 & 0 & 0 & 0 & 0 & 0 & 0 & 0 & 0 & 0 & 0 \\
0 & 0 & 0 & 0 & 0 & 0 & 0 & 0 & 0 & 2x_{8,4} & 2y_{8,4} & 2z_{8,4} & 0 & 0 \\
0 & 0 & 0 & 0 & 0 & 0 & 0 & 0 & 0 & 0 & 0 & 0 & 0 & 0 \\
0 & 0 & 0 & 0 & 0 & 0 & 0 & 0 & 0 & 0 & z_{5,7} & y_{7,5} & 0 & 0 \\
0 & 0 & 0 & 0 & 0 & 0 & 0 & 0 & 0 & z_{5,7} & 0 & x_{7,5} & 0 & 0 \\
0 & 0 & 0 & 0 & 0 & 0 & 0 & 0 & 0 & 0 & z_{8,7} & y_{7,8} & 0 & 0 \\
0 & 0 & 0 & 0 & 0 & 0 & 0 & 0 & 0 & z_{8,7} & 0 & x_{7,8} & 0 & 0 \\
0 & 0 & 1 & 0 & 0 & 0 & 0 & 0 & 0 & 0 & 0 & 0 & 0 & -d_{5.1}\sin(\theta) \\
0 & 0 & 0 & 0 & 0 & 0 & 1 & 0 & 0 & 0 & 0 & 0 & 0 & 0 \\
0 & 0 & 0 & 0 & 0 & 0 & 0 & 1 & 0 & 0 & 0 & 0 & -1 & 0 \\
0 & 0 & 0 & 0 & 0 & 0 & 0 & 0 & 1 & 0 & 0 & 0 & 0 & 0
\end{bmatrix} \tag{21}$$

Similarly, the acceleration equation is derived by differentiating the velocity Eq. (4) with respect to time. Partitioning the vector of accelerations $\ddot{\mathbf{q}}$ to $[\ddot{\mathbf{u}}^T, \ddot{\mathbf{w}}^T]^T$ where $\ddot{\mathbf{u}}$ and $\ddot{\mathbf{w}}$ are the vectors of unknown and known accelerations respectively, the acceleration

equation is expressed as,

$$[C_u]\ddot{\mathbf{u}} = [C_w]\ddot{\mathbf{w}} - ([C_q]\dot{\mathbf{q}})_q \dot{\mathbf{q}} \tag{22}$$

where the two submatrices $[C_u]$ and $[C_w]$ are defined by Eqs. (6) and (7) respectively and the square velocity term $([C_q]\dot{\mathbf{q}})_q \dot{\mathbf{q}}$ is expressed as follows,

$$[\dot{C}_q]\dot{\mathbf{q}} = \begin{bmatrix} 2\dot{x}_{5,1}^2 + 2\dot{y}_{5,1}^2 + 2\dot{z}_{5,1}^2 \\ 2\dot{x}_{5,2}^2 + 2\dot{y}_{5,2}^2 + 2\dot{z}_{5,2}^2 \\ 2\dot{x}_{6,5}^2 + 2\dot{y}_{6,5}^2 + 2\dot{z}_{6,5}^2 \\ 2\dot{x}_{7,5}^2 + 2\dot{y}_{7,5}^2 + 2\dot{z}_{7,5}^2 \\ 2\dot{x}_{7,6}^2 + 2\dot{y}_{7,6}^2 + 2\dot{z}_{7,6}^2 \\ 2\dot{x}_{8,4}^2 + 2\dot{y}_{8,4}^2 + 2\dot{z}_{8,4}^2 \\ 2\dot{x}_{9,6}^2 + 2\dot{y}_{9,6}^2 + 2\dot{z}_{9,6}^2 \\ \dot{y}_{7,5}\dot{z}_{8,4} - \dot{z}_{7,5}\dot{y}_{8,4} \\ \dot{x}_{7,5}\dot{z}_{8,4} - \dot{z}_{7,5}\dot{x}_{8,4} \\ \dot{y}_{7,4}\dot{z}_{8,4} - \dot{z}_{7,4}\dot{y}_{8,4} \\ \dot{x}_{7,5}\dot{z}_{8,4} - \dot{z}_{7,5}\dot{x}_{8,4} \\ d_{5,1}\cos(\theta)\dot{\theta}^2 \\ 0 \\ 0 \\ 0 \end{bmatrix} \tag{23}$$

Regardless the order of nonlinearity of the constraint Eq. (1), the velocity and acceleration equations are linear in terms of $\dot{q}$ and $\ddot{q}$ respectively. If the position analysis has been formulated correctly, then the matrix $[C_u]$ of a sufficient rank and becomes nonsingular. Therefore, the velocities and accelerations of the unknown points can be easily determined by solving both the linear Eqs. (5) and (8) using any numerical method. The velocities and accelerations of other points of interest can be calculated if their positions are specified. By specifying the position of the center point 10 relative to points 5, 6 and 7 of the knuckle, its position, velocity, and acceleration can be evaluated. On the other hand, the angular velocity and acceleration of the wheel knuckle link 3, or analogously of any other link in the mechanism, can be evaluated from the Cartesian coordinates, velocities, and accelerations of the three points 5, 6, and 7 defined on the

wheel knuckle as follows,

$$\omega = \frac{v_{6,5} x v_{7,5}}{v_{6,5} \cdot r_{7,5}}, \qquad \alpha = \frac{\hat{a}_{6,5} x \hat{a}_{7,5}}{\hat{a}_{6,5} \cdot r_{7,5}}$$

where $\hat{a}_{i,j} = a_{i,j} - \omega x (\omega x r_{i,j})$ and vectors $r_{i,j}, v_{i,j}$, and $a_{i,j}$ are the relative position, velocity, and acceleration vectors between points i and j. It should be noted that in this formulation, the kinematic constraints due to some common types of kinematic joints (e.g. revolute or spherical joints) can be automatically eliminated by properly locating the equivalent particles. The remaining kinematic constraints along with the geometric constraints are, in general, either linear or quadratic in the Cartesian coordinates of the particles. Therefore, the coefficients of their Jacobian matrix are constants or linear in the rectangular Cartesian coordinates. Where as in the formulation based on the relative coordinates, the constraint equations are derived based on loop closure equations which have the disadvantage that they do not directly determine the positions of the links and points of interest which makes the establishment of the dynamic problem more difficult. Also, the resulting constraint equations are highly nonlinear and contain complex circular functions. The absence of these circular functions in the point coordinate formulation leads to faster convergence and better accuracy. Furthermore, preprocessing the mechanism by the topological graph theory is not necessary as it would be the case with loop constraints. Also, in comparison with the absolute coordinates formulation, the manual work of the local axes attachment and local coordinates evaluation as well as the use of the rotational variables and the rotation matrices in the absolute coordinate formulation are not required in the point coordinate formulation. This leads to fully computerized analysis and accounts for a reduction in the computational time and memory storage. In addition to that, the constraint equations take much simpler forms as compared with the absolute coordinates. Furthermore, the use of absolute coordinates may cause numerical problems if differences of large values of the absolute coordinates are used, e.g. for the calculation of spring or damper forces or constraint residuals. The elimination of the rotational coordinates, angular velocities and angular accelerations in the presented formulation, leads to possible savings in computation time when this procedure is compared against the absolute or relative coordinate formulation. It has been determined that numerical computations associated with rotational transformation matrices and their corresponding coordinate

transformations between reference frames is time consuming and, therefore, if these computations are avoided more efficient codes may be developed. The elimination of rotational coordinates can also be found very beneficial in design sensitivity analysis of multibody systems. In most procedures for design sensitivity analysis, leading to an optimal design process, the derivatives of certain functions with respect to a set of design parameters are required. Analytical evaluation of these derivatives are much simpler if the rotational coordinates are not present and if we only deal with translational coordinates. Some practical applications of multibody dynamics require one or more bodies in the system to be described as deformable in order to obtain a more realistic dynamic response. Deformable bodies are normally modeled by the finite element technique. Assume that the deformable body is connected to a rigid body described by a set of particles. Then, one or more particles of the rigid body can coincide with one or more nodes of the deformable body in order to describe the kinematic joint between the two bodies. This is a much simpler process that when the rigid body is described by a set of translational and rotational coordinates. In general, the point coordinates have additional advantages over the other systems of coordinates since they are the most suitable coordinates for the graphics routines and the animation programs. It should be mentioned that there is no single multibody formulation to be considered as the best formulation for general mechanical systems. Each formulation has its own unique or common features and, therefore, selected features should be adopted to our advantages.

2.3. Numerical Example. Since the position analysis is a nonlinear problem which is solved by an iterative numerical method, it is expected that the problem of multiple solutions arrises. In order to avoid such problem, knowing the input driving variables, measurements can be used initially to obtain a good initial guess at the starting point of the position analysis. In the subsequent iterations, the problem of multiple solution can be overcome taking as a good initial guess the previous configuration of the system. The initial position of the mechanism is given by the initial coordinates of the assigned points listed in Table 1. The chassis is assumed stationary and therefore the values of the velocities and accelerations of all known points fixed on it are identically zero. The driving variables θ and S are taken as functions of time in the form, $\theta(t) = 0.8 + 0.25t + 0.0625t^2$ and $S(t) = 0.15t + 0.0025t^2$, respectively. Given the known

coordinates, the 15 nonlinear equations of constraints given by Eq. (1), are solved by the Newton-Raphson's method of successive approximation to determine the 15 unknown Cartesian coordinates for different time steps. Then the velocity Eq. (5) and acceleration Eq. (8) are solved for the unknown Cartesian velocities and accelerations of the unknown points for different time steps using the L-U factorization with pivoting method. It is recommended here to consider each of the two driving variables separately in order to study their effect clearly.

a) Effect of the driving rotation variable $\theta(S = 0)$:

Table 2 illustates the effect of the driving rotation variable θ on the Cartesian coordinates of the wheel centre point 10 and the angular velocity and acceleration of the knuckle. Since the rotation of the lower arm by an angle θ causes a sliding motion of the strut sliding joint along the axis AD, the variation of the vertical displacement of the wheel centre point in the z direction is the most dominant. The time variations of the kingpin as well as the camber angles and the vertical displacement of the wheel centre point are, respectively, presented in Figs. 5 and 6.

b) Effect of the sliding variable S $(\theta = 90^o)$:

Table 3 illustrates the effect of the driving sliding variable S on the Cartesian coordinates of the wheel centre point 10 and the angular velocity and acceleration of the wheel knuckle. The sliding motion of the rack causes the rotation of the strut and the wheel about the steering axis AD. By increasing the sliding displacement S, the x-coordinate of the centre point decreases. The decrease of the x-coordinate is the most dominant change in the coordinates of the centre point. Figures 7 and 8, respectively, indicate the time variations of the kingpin as well as the camber angles and the vertical displacement of the wheel centre point. It should be noted that the results of the simulation are tested and compared with the simulation based on absolute coordinates formulation. The comparison shows a complete agreement between the two formulations.

3. CONCLUSIONS

In this paper, a numerical algorithm for the kinematic analysis of the spatial two DOF multi-loop MacPherson strut suspension mechanism is presented. The kinematic analysis is carried out in terms of the rectangular Cartesian coordinates of some defined points in the links and at the kinematic joints. The present formulation accommodates

all types of basic kinematic joints; revolute, prismatic, and spherical joints. Because of the presence of the strut prismatic joint, the kinematic constraints are added to the geometric constraints in the formulation. Additional driving constraints are included as functions of the two input driving variables. The suggested algorithm eliminates the need to write redundant constraints and allows the solution of a reduced system of equations. The results of the analysis indicate the simplicity and generality of the proposed algorithm.

REFERENCES

[1] Wehage, R.A. and Haug, E.J., "Generalized Coordinate Partitioning of Dimension Reduction, in Analysis of Constrained Dynamic Systems," ASME Journal of Applied Mechanical Design, Vol. 104, pp. 247-255, 1982.

[2] Nikravesh, P.E., Computer-Aided Analysis of Mechanical Systems, Prentice-Hall, 1988.

[3] Denavit, J. and Hartenberg, R.S., "A Kinematic Notation for Lower-Pair Mechanisms Based on Matrices", ASME Journal of Applied Mechanics, pp. 215-221, 1955.

[4] Paul, B. and Krajcinovic, D., "Computer Analysis of Machines with Planar Motion-1. Kinematics, 2. Dynamics," ASME Journal of Applied Mechanics, Vol. 37, pp. 697-712, 1970.

[5] Cronin, D.L., "MacPherson Strut Kinematics," Mechanism and Machine Theory, Vol. 16, pp. 631-644, 1981.

[6] Garcia de Jalon, J., Serna, M. A., and Aviles, R., "Computer Method for Kinematic Analysis of Lower-Pair Mechanisms-I Velocities and Accelerations", Mechanism and Machine Theory, Vol. 16, pp. 543-556, 1981.

[7] Garcia de Jalon, J., Serna, M.A., and Aviles, R., "Computer Method for Kinematic Analysis of Lower-Pair Mechanisms-II Position Problems", Mechanism and Machine Theory, Vol. 16, pp. 557-566, 1981.

[8] Garcia de Jalon, J. et al., "Simple Numerical Method for the Kinematic Analysis of Spatial Mechanisms", ASME Journal on Mechanical Design, Vol. 104, pp. 78-82, 1982.

[9] Vilallonga, G., Unda, J., and Garcia de Jalon, J., "Numerical Kinematic Analysis of Three-Dimensional Mechanisms Using a 'Natural' System of Lagrangian Coordinates," ASME Paper No. 84-DET-199, 1984.

[10] Akhras, R. and Angeles, J., "Unconstrained Nonlinear Least-Square Optimization of Planar Linkages for Rigid-Body Guidance," Mechanism and Machine Theory, Vol. 25, pp. 97-118, 1990.

[11] Attia, H.A., A computer-Oriented Dynamical Formulation with Applications to Multibody Systems, Ph.D. Dissertation, Department of Engineering Mathematics and Physics, Faculty of Engineering, Cairo University, 1993.

[12] Garcia de Jalon, J. and Bayo, E., "Kinematic and dynamic simulation of multibody systems: The real-time challenge", Springer-Verlag, New York, 1994.

[13] Attia, H.A., "Numerical Kinematic Analysis of the Double Wishbone Motor-Vehicle Suspension System," CSME Transactions, Vol. 24, No. 2, pp. 391-399, 2000.

[14] Molian, S., "Solution of Kinematics Equations by Newton's Method," Journal of Mechanical Engineering Science, Vol. 10, No. 4, pp. 360-362, 1968.

[15] Adler, U., Automotive Handbook, Bosch, FDI-Verlag, Approved Edition Under Licence SAE, ISPN 089283-518-6.
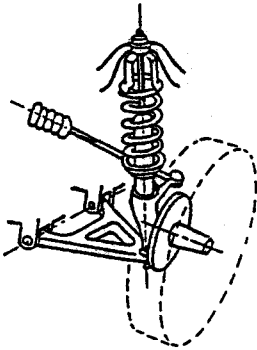
Fig. 1 The MacPherson strut suspension system [5].
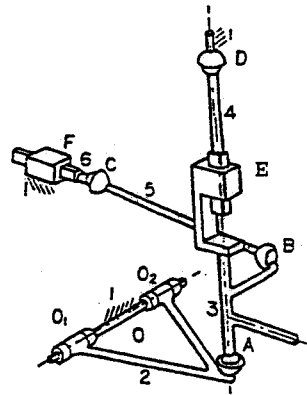
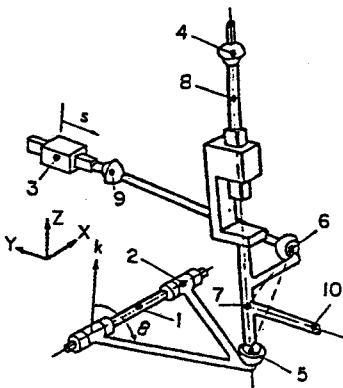**Fig. 2 The MacPherson strut mechanism [5].**

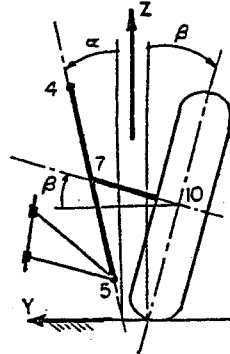**Fig. 3 The MacPherson strut with the assigned points.**
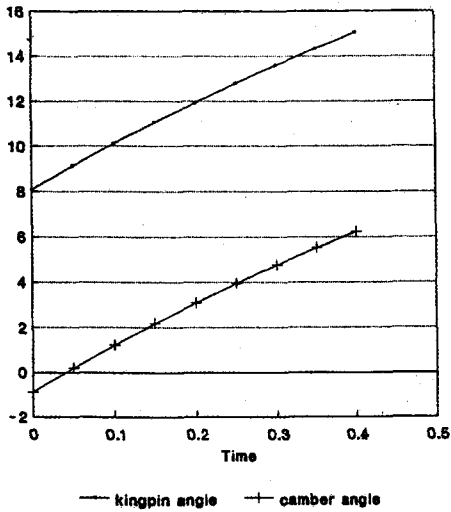

Fig. 4 Kingpin and camber angles.

Fig. 5 Time (s) variation of the
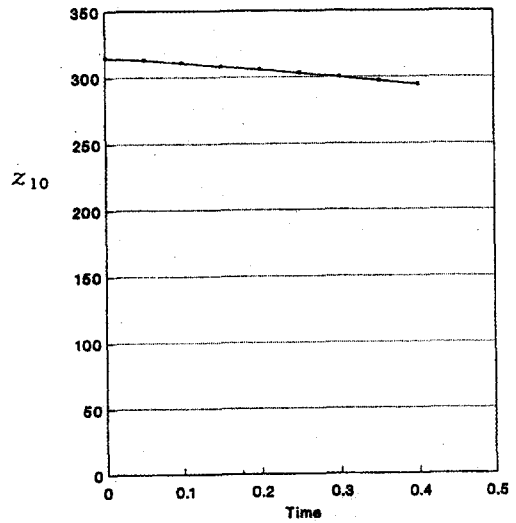Kingpin and camber angles (Deg)
for $S = 0$

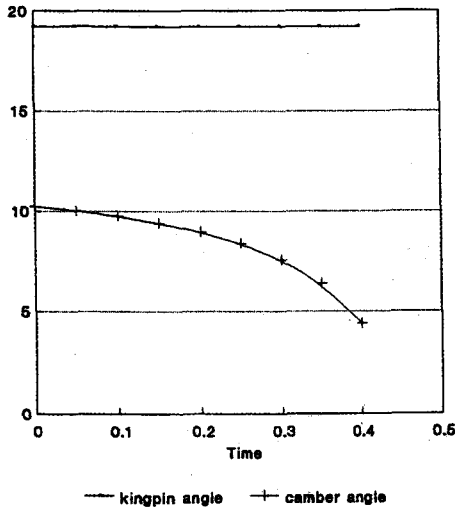Fig. 6 Time (s) variation of
z_{10} (mm) for $S = 0$

Fig. 7 Time (s) variation of the
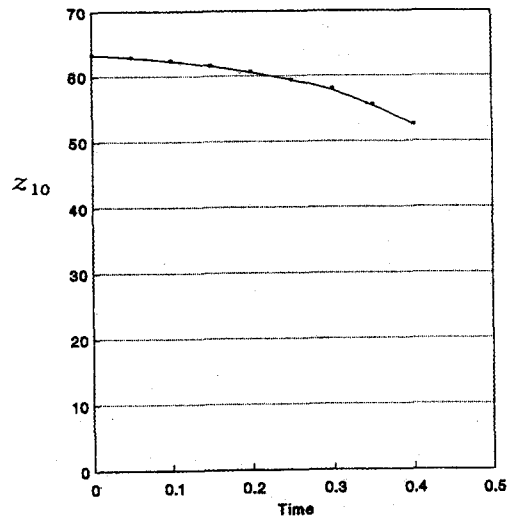Kingpin and camber angles (Deg)
for $\theta = 90°$

Fig. 8 Time (s) variation of
z_{10} (mm) for $\theta = 90°$

Table 1 Initial Cartesian coordinates (mm) of the points

(x_1,y_1,z_1)	$(270,-5,-10)$	(x_6,y_6,z_6)	$(560,-300,60)$
(x_2,y_2,z_2)	$(540,-10,-20)$	(x_7,y_7,z_7)	$(452,-320,20)$
(x_3,y_3,z_3)	$(570,60,90)$	(x_8,y_8,z_8)	$(456,-250,246)$
(x_4,y_4,z_4)	$(460,-180,470)$	(x_9,y_9,z_9)	$(570,60,90)$
(x_5,y_5,z_5)	$(450,-330,-40)$	(x_{10},y_{10},z_{10})	$(452,-410,20)$

Table 2 Simulation results for $S=0$

Time (s)	θ (deg)	(x_{10},y_{10},z_{10}) (mm)	$\omega_{knuckle}$ (rad/s)	$\alpha_{knuckle}$ (rad/s^2)
0.0	45.84	$(451,-291,315)$	$-(0.4,0.03,0.3)$	$(0.3,-0.05,0.39)$
0.2	48.85	$(446,-305,305)$	$-(0.3,0.04,0.2)$	$(0.33,0.003,0.3)$
0.6	55.72	$(440,-334,277)$	$(0.2,-0.04,-0.1)$	$(0.31,0.06,0.25)$
1.0	63.74	$(437,-364,234)$	$(-0.1,0.01,0.02)$	$(0.26,0.1,0.198)$
1.2	68.18	$(436,-378,208)$	$(-0.03,0.02,0.1)$	$(0.2,0.07,0.18)$
1.6	77.92	$(437,-401,146)$	$(0.05,0.05,0.12)$	$(0.19,0.05,0.1)$
2.0	88.81	$(440,-415,71.6)$	$(0.12,0.06,0.17)$	$(0.15,0.01,0.1)$
2.2	100.8	$(444,-412,-12)$	$(0.18,0.058,0.2)$	$(0.13,-0.03,0.04)$
2.6	107.3	$(447,-404,-57)$	$(0.2,0.05,0.21)$	$(0.13,-0.1,-0.02)$

Table 3 Simulation results for $\theta=90^\circ$

Time (s)	S (mm)	(x_{10},y_{10},z_{10}) (mm)	$\omega_{knuckle}$ (rad/s)	$\alpha_{knuckle}$ (rad/s^2)
0.00	0.00	$(440.4,-415,63)$	$(0.03,0.2,0.617)$	$-(0.04,0.27,0.77)$
0.05	7.56	$(434,-415,63.5)$	$-(0.09,0.66,1.9)$	$-(1.82,14.2,40.7)$
0.10	15.25	$(427,-414,63.5)$	$-(0.01,0.06,0.2)$	$-(0.09,0.67,1.92)$
0.15	23.06	$(420,-413,63.3)$	$-(0.004,0.03,0.1)$	$(0.009,0.07,0.2)$
0.20	31.00	$(413.7,-411,63)$	$(-0.18,0.14,0.4)$	$(0.197,1.54,4.4)$
0.25	39.06	$(407,-409,62.4)$	$(0.8,-0.76,-1.4)$	$(1.4,-5.57,-9.7)$
0.30	47.25	$(400.4,-406,62)$	$(0.3,-0.24,-0.3)$	$-(1.73,0.98,2.51)$
0.35	55.56	$(394,-402,60.7)$	$-(4.1,0.53,6.9)$	$(115.3,51.8,269)$
0.40	64.00	$(389,-398,-60)$	$-(0.37,1.6,4.78)$	$(0.526,1.94,4.9)$

Dept. of Math.,

College of Science,

KIng Saud University (Al-Qassem Branch),

Egypt